ACS OMEGA

http://pubs.acs.org/journal/acsodf

Article

Enrichment in CO_2 Absorption by 2-Methyl Piperazine-Activated Tertiary Amines, Physical Solvents, and Ionic Liquid Systems

Sweta C. Balchandani, Bishnupada Mandal,* and Swapnil Dharaskar

Cite This: *ACS Omega* 2022, 7, 23611−23623

Read Online

ACCESS | Metrics & More | Article Recommendations | Supporting Information

ABSTRACT: One of the ever-demanding research fields is the development of new solvents with better properties for mitigation of CO_2 compared to existing solvents. This work reports the measurement and modeling of CO_2 solubility in newly proposed aqueous solvent blends of 2-methyl piperazine with *N*-methyldiethanolamine (MDEA), sulfolane ($TMSO_2$), and 1-butyl-3-methyl-imidazolium acetate ([bmim] [Ac]). The operating temperature and CO_2 partial pressure conditions chosen were 303.2−323.2 K and 2−370 kPa, respectively. Along with this, qualitative ^{13}C NMR and FTIR analysis were also performed to consider the proposed reaction scheme. The experimental vapor−liquid equilibrium data were modeled by a modified Kent−Eisenberg equilibrium model. The equilibrium constants associated with 2-methyl piperazine (2-MPZ) and [bmim] [Ac] deprotonation and carbamate formation reactions were regressed to fit the experimental CO_2 solubility data. In addition, the CO_2 cyclic capacity and heat of absorption were evaluated for the aq (MDEA + 2-MPZ) blend.

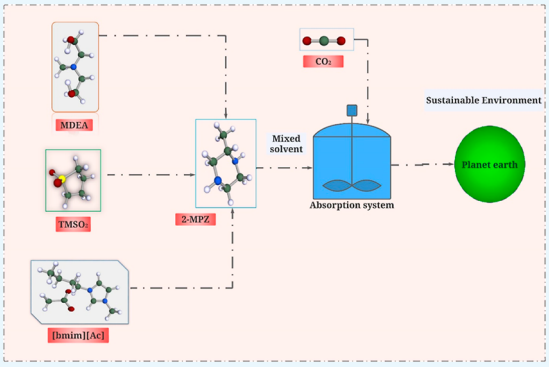

1. INTRODUCTION

The current requirement of mass absorption of various greenhouse gases is an essential controlling action for mitigating climate changes. Of the many greenhouse gases emitted into the atmosphere, CO_2 is the largest anthropogenic gas; hence, its control in the energy sector has been an ever-expanding issue for decades. Although post-combustion CO_2 capture is a mature technology, new advanced trends are being proposed for the betterment of the existing solution. One of the key areas of research is the development of new solvents with essential properties such as high reaction rates, high CO_2 solubility, environmental friendliness, high CO_2 cyclic capacity, low heat of absorption, high thermal stability, low solvent cost, and less regeneration energy.[1−4] Most of these properties cannot be obtained using a single solvent, hence blends of various categories of solvents that aid CO_2 absorption are explored for the purpose. It is also proposed that provided a solvent works well for post-combustion CO_2 capture, it will definitely result in high CO_2 absorption in pre-combustion processes because of the fact that, usually, the pre-combustion inflow streams are rich in CO_2 concentration.

Recently, the possible application of deep eutectic solvents with the aim of achieving lower regeneration energy has also been reported.[5] Usually, the synthesis of deep eutectic solvents is energy- and cost-intensive. However, the method suggested by the authors proved to be very cost-effective, yielding desired results for high CO_2 solubility. The CO_2 solubility in several aqueous amines such as monoethanolamine (MEA),[6] *N*-methyldiethanolamine (MDEA),[7] diethanolamine (DEA),[8] and 2-amino-2-methyl-1-propanol (AMP)[9] has been studied in the literature over an extensive range of temperatures, pressures, and concentrations. Nevertheless, due to either low-equilibrium CO_2 solubility or low reaction rates of these amines, addition of activators is recommended by many researchers.[10,11] Various activators such as piperazine and its derivatives blended with AMP,[11] MDEA,[12] MEA,[13] and potassium carbonate (K_2CO_3)[14] have been widely considered in the literature. Other amine activators which have been studied and proposed for the said purpose are bis (3-aminopropyl) amine (APA), hexamethylenediamine, and triethylenetetramine.[15−18] One of the PZ derivatives, viz., 2-methyl piperazine (2-MPZ), is explored in the present study for CO_2 absorption. A brief literature review of the selected solvents is discussed in the subsequent text.

The performance of CO_2 loading in potassium carbonate while increasing the concentration of amine additives such as 2-MPZ, potassium sarcosinate, and potassium lysinate has been investigated and reported in the literature, and it was observed that the inclusion of 2-MPZ and potassium lysinate has an affirmative influence on the CO_2 solubility.[19] Nevertheless, the temperature 313.15 K and the pressure range 0−50 kPa were quite narrow in comparison to the horizon of CO_2

Received: April 9, 2022
Accepted: June 15, 2022
Published: June 30, 2022

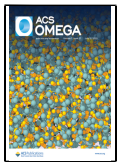

absorption applications. The highest CO_2 loading found at 50 kPa with a molar fraction of 0.4 of 2-MPZ in K_2CO_3 solution was evaluated to be 0.89.

The simulation analysis of CO_2 absorption in aqueous activator blends of PZ/2-MPZ for varying concentrations has also been reported over a wide range of temperatures and pressures using Aspen Plus. The blends were investigated for CO_2 solubility where a meticulous analysis of speciation, kinetic parameters, and heat of absorption was done using the e-NRTL model.[20] The highest CO_2 loading capacity for (4 *m* piperazine + 4 *m* 2-MPZ) was found to be 0.84 mol of CO_2/(kg amine + H_2O), which is reasonably competitive with traditionally used aqueous amines. Similar studies of PZ/2-MPZ have also been reported elsewhere.[21−24] The precipitation of piperazine at lower temperatures leads to the search for new activators that offer better absorption rates and cyclic capacity. The selection of the optimum concentration ratio of PZ/2-MPZ is also a huge concern since an increase in the concentration of 2-MPZ increases the viscosity of the overall system and thereby decreases the CO_2 solubility due to less diffusion. 2-MPZ and PZ have also been investigated as promoters for K_2CO_3, and it was concluded that (15 wt % K_2CO_3 + 10 wt % 2-MPZ + 10 wt % PZ) at 313.15 K exhibits the highest CO_2 loading and absorption rates.[14]

Pure physical solvents, such as sulfolane ($TMSO_2$), *N*-methylpyrrolidone (NMP), propylene carbonate (PC), etc., and their aqueous solvents have also been preferred over the years owing to the advantage of extremely low vapor pressure, leading to a low energy requirement in the regeneration step for acid gas separation systems.[25−27] However, due to the low-equilibrium CO_2 solubility and requirement of high pressures of the input streams for effective absorption, the blended solutions of physical solvents with amines have been reported in the literature.[28] The thermodynamic analysis of the simultaneous removal of mercaptans and CO_2 in aq ($TMSO_2$ + DIPA) and aq ($TMSO_2$ + MDEA) systems using PC-SAFT and e-NTRL models has also been reported.[29] The results indicated that the studied solvents performed better than aq $TMSO_2$ solutions. The effect of the increase in the PZ concentration in the blends of aq (MDEA + $TMSO_2$) is also reported in the literature.[12] The composition (42 wt % MDEA + 8 wt % PZ + 10 wt % $TMSO_2$) is indicated to yield the highest CO_2 solubility of α_{CO2} = 1.21163 mol of CO_2/mol of (MDEA + PZ) at 303.15 K and 1236.604 kPa,[12] which is comparable to traditionally used primary and secondary amines with PZ.

Recently, the simultaneous removal of CO_2 and ethyl mercaptans has also been reported using aq (MDEA + $TMSO_2$) solutions.[30] The experimental results inferred that with increment in MDEA concentration from 30 to 40% at a constant total concentration of the solvent at 328.15 K, there was an increase in CO_2 solubility of about 28.30%. Biphasic solvent mixtures of H_2O, diethylenetriamine, and $TMSO_2$ have proved to be competitive with the blends of MDEA, $TMSO_2$, and H_2O under similar experimental conditions with respect to CO_2 solubility and kinetics of the systems.[31,32] Although a general conclusion states that most of the carbamate, dicarbamate, and tricarbamate are formed due to the amine phase rather than the $TMSO_2$ phase.

In addition, another category of solvents that has been extensively studied over the past few decades is ionic liquids, owing to the better solvent properties they offer in comparison to amines. On the other hand, ILs also tend to exhibit lower CO_2 absorption. Hence, blends of amines or amine activators with ILs may prove to increase the efficiency of the CO_2 absorption/desorption process.[33,34] Imidazolium-based ILs are well established in the literature,[35−37] proving them to be more cost-competitive and having higher CO_2 absorption in comparison to phosphonium- or pyridinium-based ILs. 1-Butyl-3-methylimidazolium acetate ([bmim] [Ac]) activated by amine activators 1-(2-aminoethyl) piperazine (AEP), and bis(3-aminopropyl)amine (APA), is also one of the promising solvents for CO_2 capture, which was earlier reported by our group.[38]

Conclusively, aqueous blends of MDEA, $TMSO_2$, and [bmim] [Ac], that is, a tertiary amine, a physical solvent, and an ionic liquid with 2-MPZ (amine activator), respectively, have been envisioned as potential solvents for CO_2 capture. The concentration of the chemicals involved in the measurement of CO_2 equilibrium solubility has been chosen rationally to get the desired optimum results. Subsequently, the vapor−liquid equilibrium (VLE) data have also been correlated using the Kent−Eisenberg model for CO_2 solubility in aq (MDEA + 2-MPZ), aq ($TMSO_2$ + 2-MPZ), and aq ([bmim] [Ac] + 2-MPZ). The efficacy of the studied solvents for CO_2 absorption has been confirmed by COSMO-RS theoretical analysis and has been reported elsewhere.[39]

2. EXPERIMENTAL SECTION

2.1. Materials. CO_2 gas (>99% pure) was procured from Linde India Ltd. and used without further purification. [bmim] [Ac] (≥95% pure), $TMSO_2$ (99% pure), 2-MPZ (95% pure) and MDEA (≥99% pure) were purchased from Sigma-Aldrich. $TMSO_2$, 2-MPZ, and MDEA were used with no auxiliary refinement for the CO_2 solubility study. For solution preparation, the [bmim] [Ac] was first analyzed for its initial water content by the Karl Fischer method, which was found to be 1.7%. Then, the solvent was vacuum-dried for 48 h and analyzed again for water content, which was then calculated to be 0.04%. The solvent systems were prepared using double-distilled deionized water. Specification details of the chemicals used in this study were reported elsewhere.[39]

2.2. Experimental Method. *2.2.1. VLE Measurement.* The schematic of the experimental setup, methodology, and validation of the assembly used to measure the VLE has been reported in detail by our research group.[38,40,41] However, the measurement method and calculation of equilibrium data are briefly described here. The setup consists of two cells: a buffer (for storage of CO_2 gas at a specific temperature and pressure) and an equilibrium cell (for reaction). Both the cells are equipped with temperature and pressure controllers and transducers in order to change and track the differences in temperature and pressure. The solvent introduced in the equilibrium cell is continuously stirred with the help of a magnetic stirrer. The total pressure (P^T) prevailing in the equilibrium vessel and solvent vapor pressure (P^v) can be used to evaluate the equilibrium partial pressure of CO_2 (P_{CO2}) at the respective temperature and liquid phase CO_2 loading (α). The CO_2 loading (α_{CO2}) was further estimated as a function of temperature and P_{CO2}. A similar method has been used in the literature for the measurement of CO_2 equilibrium capacity.[42−48] Other approaches such as the wetted wall column method[49,50] and the Rubotherm magnetic suspension balance method[51,52] have been reported in the literature for CO_2 solubility. The wetted wall column method is primarily used for establishing the kinetics of the CO_2 absorption

https://doi.org/10.1021/acsomega.2c02217
ACS Omega 2022, 7, 23611−23623

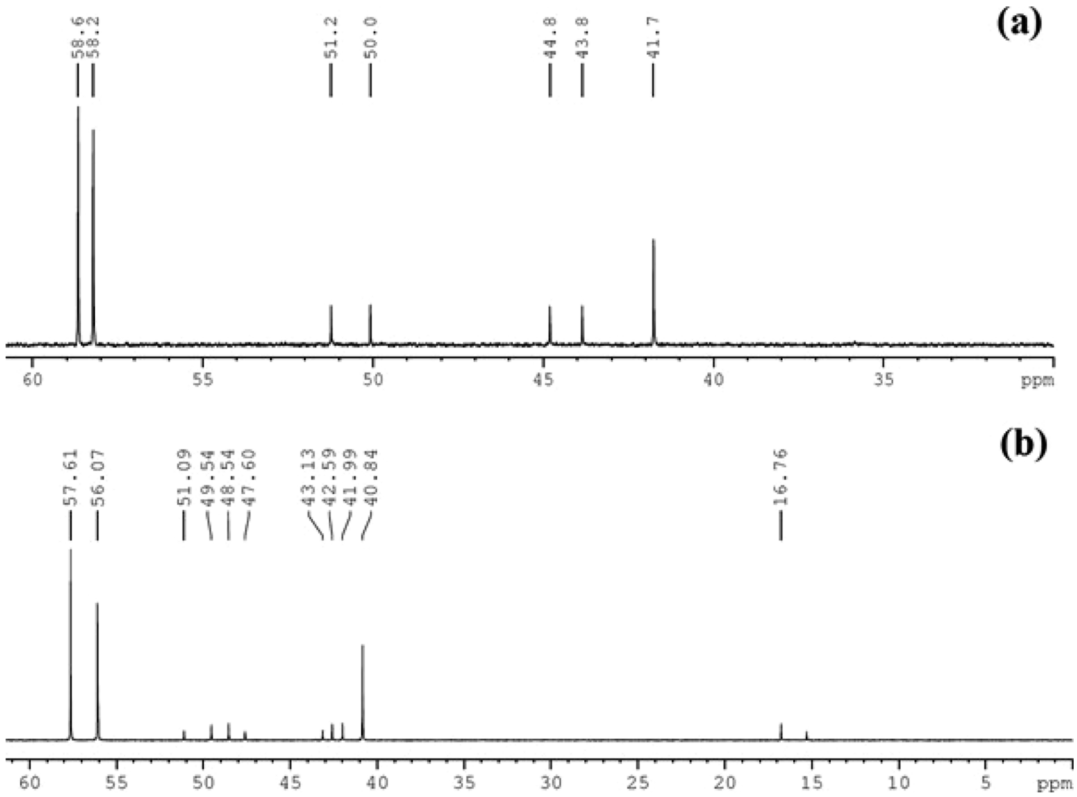

Figure 1. ^{13}C NMR spectra of aq (3.017 *m* MDEA + 1.008 *m* 2-MPZ) solution (a) unloaded and (b) CO_2 loaded at 313.2 K.

process. However, through the graphical method using the mass transfer coefficient and CO_2 partial pressure in the bulk phase, the CO_2 equilibrium partial pressure can be evaluated as function of CO_2 loading and temperature. Furthermore, the Rubotherm magnetic suspension balance method is quite costly. The approach is based on changes in weight calculations while CO_2 absorption takes place and is principally used for the screening of expensive solvents such as ionic liquids. Contrastingly, the equilibrium cell methodology adopted for the current work of CO_2 absorption is less cumbersome and reasonably priced.

The detailed equations required for calculations of α_{CO2} and associated uncertainty[53,54] are represented in Table S1. Nine solvents with the following compositions are studied in the present work at 303.2, 313.2, and 323.2 K (1) aq (3.509 *m* MDEA + 0.509 *m* 2-MPZ), (2) aq (3.017 *m* MDEA + 1.008 *m* 2-MPZ), (3) aq (2.502 *m* MDEA + 1.509 *m* 2-MPZ), (4) aq (3.501 *m* $TMSO_2$ + 0.509 *m* 2-MPZ), (5) aq (3.012 *m* $TMSO_2$ + 1.008 *m* 2-MPZ), (6) aq (2.500 *m* $TMSO_2$ + 1.509 *m* 2-MPZ), (7) aq (3.507 *m* [bmim] [Ac] + 0.509 *m* 2-MPZ), (8) aq (3.002 *m* [bmim] [Ac] + 1.008 *m* 2-MPZ), and (9) aq (2.510 *m* [bmim] [Ac] + 1.509 *m* 2-MPZ). Here, "*m*" represents mol/kg (molal unit).

2.2.2. FTIR and ^{13}C NMR Analyses. The ^{13}C NMR spectra of the CO_2 unloaded and loaded aq (3.017 *m* MDEA + 1.008 *m* 2-MPZ) blend were carried out using a 500 MHz NMR spectrophotometer in D_2O (model: Ascend, Bruker). The FTIR-ATR spectra (PerkinElmer Inc., Germany) has also been performed to qualify the system analysis in the range of 1800 to 600 cm^{-1}.

Qualitative ^{13}C NMR and FTIR-ATR studies are performed to confirm various products of formation during the reaction of solvents under study with CO_2. The majority of new peaks formed due to CO_2 loading were observed in the up field of ^{13}C NMR spectra (Figure 1). The peaks at 16.76−43.13 associated with several CH_2 groups of intermediate reactive species correspond to MDEA. However, on the other hand, peaks at 47.60−57.61 correspond to various mono- and secondary-carbamates formed in the system due to the presence of 2-MPZ.[15,16,55,56]

The FTIR-ATR analysis of the aq (3.017 *m* MDEA + 1.008 *m* 2-MPZ) system under unloaded and under CO_2 loading conditions at 313.2 K is carried out (Figure 2). The characteristic peaks have been identified and apportioned as presented in Table 1 conclusive of which protonation of MDEA and different carbamate species formations have been inveterate.

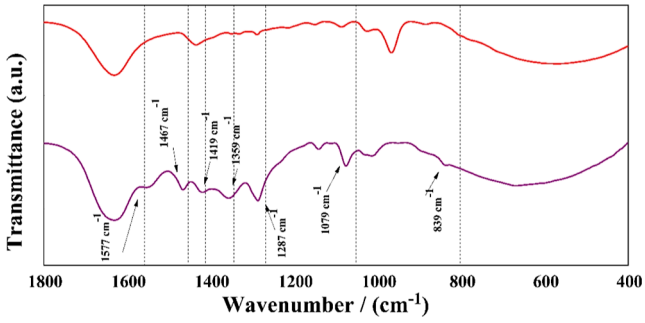

Figure 2. FTIR-ATR spectra of aq (3.017 *m* MDEA + 1.008 *m* 2-MPZ): red line, unloaded, and purple line, CO_2 loaded at 313.2 K.

3. PROPOSED CHEMICAL REACTION

Through the results obtained in ^{13}C NMR and FTIR studies and literature[20−22,38] for 2-MPZ, the equilibrium reactions for

https://doi.org/10.1021/acsomega.2c02217
ACS Omega 2022, 7, 23611−23623

Table 1. FTIR-ATR Peaks and Their Ascription in aq (3.017 *m* MDEA + 1.008 *m* 2-MPZ) at 313.2 K

Sl. no.	wavenumber (cm^{-1})	attribution
1	839	C−NH_2 twisting for 2-MPZ
2	1079	protonation of MDEA to form $MDEAH^+$
3	1287	N−C stretching vibration of 2-MPZ carbamate
4	1359	HCO_3^-
5	1419	asymmetric and symmetric vibrations of COO^- of 2-MPZ monocarbamate
6	1467 and 1577	asymmetric and symmetric stretching of COO^-

aq (MDEA + H_2O + CO_2 + 2-MPZ), aq ($TMSO_2$ + H_2O + CO_2 + 2-MPZ), and aq ([bmim] [Ac] + H_2O + CO_2 + 2-MPZ) systems and the equilibrium constants associated with each reaction are proposed in this work (Table S2). The physical solubility of CO_2 is presented here by Henry's law. Reversible reactions in the liquid phase are explained using chemical reaction equilibrium constants through the conceptualization of chemical equilibrium. The liquid phase reaction consists of protonation of both MDEA and 2-MPZ amine activators, carbamate formation by 2-MPZ and [bmim] [Ac], and several other reactions of formation of bicarbonate or carbonate species. The bicarbamate formation of 2-MPZ has not been reflected in the present study because at higher α_{CO2} bicarbonate is the key product of (2-MPZ-CO_2) reaction.[22] The carbamate formation for the reaction between [bmim] [Ac] and CO_2 has been already reported in the literature.[35,38,57] Since $TMSO_2$ is a physical solvent, it is assumed to exhibit negligible chemical interactions and only may have weak van der Waals forces of attraction with CO_2 and other species in the system. For all the systems considered in this work, the following reactions are in common: physical solubility, formation of bicarbonate ion, dissociation of bicarbonate ion, and dissociation of water. The chemical reactions pertaining to the [bmim] [Ac] + CO_2 + H_2O system have been reported by our research group elsewhere.[38] It has also been confirmed through the experimental data, FTIR, and ^{13}C NMR studies that [bmim] [Ac] having two active amino groups undergoes deprotonation and carbamate hydrolysis reaction.[38] MDEA, being a tertiary amine and having one amino group, offers only deprotonation reaction in the MDEA + CO_2 + H_2O system.[58,59] Furthermore, $TMSO_2$ is a well known physical solvent used for solubilizing CO_2.[26] Using the ^{13}C NMR spectra, Chen et al. suggested the detailed reaction mechanism of the 2-MPZ + H_2O + CO_2 system.[21,22] As per the published study, there are two amino groups in the 2-MPZ structure, out of which one of the amino groups stands in hindrance due to the presence of the neighboring methyl group. Both the amino groups form monocarbamate—one is hindered and the other unhindered. However, the electron-giving methyl group is anticipated to ease the positive charge on the adjoining amino group, so the protonation is likely to strike first on the hindered amino group. Both the 2-MPZ carbamates further can be either protonated and form zwitterions or react with one more CO_2 to form dicarbamate. Consequently, for the current work, two major reactions offered by 2-MPZ are considered: deprotonation and carbamate hydrolysis. Hence, the enhancement of CO_2 solubility is majorly due to the presence of 2-MPZ and the reactions offered by 2-MPZ, along with the base solvents of MDEA, [bmim] [Ac], and $TMSO_2$.

4. VLE MODELING

Efficient correlation of CO_2 solubility in solvents has been approached in different manners in the literature. Usually, if pure ionic liquids or physical solvents are utilized as CO_2 absorbents, the system is modeled using the equation of states, such as Peng−Robinson, Redlich−Kwong, and so forth, with different mixing rules, including cubic and group contribution methods.[60] However, amines used for the CO_2 absorption process are usually modeled by complex models such as Clegg−Pitzer,[61] e-NRTL,[12] Deshmukh−Mather,[62] and Kent−Eisenberg.[63−65] Of the many available models, the Kent−Eisenberg model exhibits several advantages over other models in that it does not require various essential characteristics of the solvents, such as critical temperature, critical or reduced pressures, boiling point, binary interaction parameters, and acentric factors. Originally, in the KE model, equilibrium constants of the reactions participating in the system were considered to be a function of a single variable, that is, temperature.[66] Later on, due to the complex behavior of the CO_2 solubility in any solvent system, the attributes of concentration of solvents and CO_2 partial pressure were also included as variables during the estimation of equilibrium constants. One of the major advantages of the modified KE model is that it allows the estimation of various species and pH in the system easily. Hence, more knowledge can be gained regarding the behavior of the system under study. In the present work, all the systems have been correlated using a modified KE model.

Henry's law signifies the relationship between the CO_2 partial pressure P_{CO2} at equilibrium and the physically dissolved CO_2 concentration [CO_2] to describe the vapor phase equilibrium, which is presented in eq 1.

$$P_{CO_2} = H_{CO_2} \times [CO_2] \tag{1}$$

The modified KE model derivation for the ([bmim] [Ac] + H_2O + CO_2 + 2-MPZ) system is presented here. The model has already been presented for similar systems in our earlier work.[38,40,41,67]

For simplification, [bmim] [Ac] is renamed as R_1. The general mass and charge balance of various molecular and ionic species in the liquid phase is presented as follows

[bmim] [Ac] balance

$$[R_1]_t = M_1 = [R_1] + [R_1H^+] + [R_1COO^-] \tag{2}$$

2-MPZ balance

$$\begin{aligned}[2-\mathrm{MPZ}]_t &= M_2 \\ &= [2-\mathrm{MPZ}] + [2-\mathrm{MPZH}^+] \\ &\quad + [2-\mathrm{MPZCOO}^-]\end{aligned} \tag{3}$$

CO_2 balance for the aq [bmim] [Ac] +2-MPZ system

$$\begin{aligned}&\alpha_{CO_2} \times (M_1 + M_2) \\ &= [CO_2] + [HCO^{3-}] + [CO_3^{2-}] + [R_1COO^-] \\ &\quad + [2-\mathrm{MPZCOO}^-]\end{aligned} \tag{4}$$

Electroneutrality balance/charge balance for the aq ([bmim] [Ac] + 2-MPZ) system

https://doi.org/10.1021/acsomega.2c02217
ACS Omega 2022, 7, 23611−23623

Table 2. CO_2 Solubility Data in aq (MDEA + 2-MPZ) Solution[a]

aq (MDEA+ 2-MPZ)	T = 303.2 K		T = 313.2 K		T = 323.2 K	
molal (m)	P_{CO2}/kPa	α_{CO2}	P_{CO2}/kPa	α_{CO2}	P_{CO2}/kPa	α_{CO2}
3.509 + 0.509	4.3	0.189 ± 0.002	5.7	0	6.6	0.139 ± 0.001
	9.8	0.331 ± 0.002	15.2	0.335 ± 0.003	18.1	0.270 ± 0.002
	21.2	0.462 ± 0.003	40.3	0.459 ± 0.004	33.8	0.376 ± 0.003
	41.2	0.569 ± 0.004	72.7	0.546 ± 0.005	56.1	0.454 ± 0.004
	65.1	0.644 ± 0.005	90.5	0.605 ± 0.005	73.6	0.513 ± 0.005
	98.5	0.683 ± 0.006	114.3	0.642 ± 0.006	99.4	0.548 ± 0.005
	119.1	0.708 ± 0.007	133.7	0.671 ± 0.007	114.2	0.578 ± 0.006
	143.1	0.722 ± 0.007	157.8	0.761 ± 0.008		
	197.3	0.749 ± 0.009	199.3	0.775 ± 0.009		
	203.2	0.753 ± 0.009				
3.017 + 1.008	2.3	0.183 ± 0.001	5.0	0.155 ± 0.001	5.0	0.141 ± 0.001
	10.1	0.345 ± 0.002	11.5	0.303 ± 0.002	15.1	0.300 ± 0.002
	20.0	0.506 ± 0.004	27.0	0.435 ± 0.003	34.5	0.422 ± 0.003
	44.5	0.627 ± 0.005	57.9	0.534 ± 0.004	72.0	0.494 ± 0.004
	86.5	0.706 ± 0.006	77.6	0.596 ± 0.005	82.9	0.554 ± 0.005
	118.8	0.737 ± 0.007	99.2	0.638 ± 0.006	104.0	0.596 ± 0.006
	146.2	0.759 ± 0.007	116.9	0.670 ± 0.006	129.6	0.624 ± 0.006
	183.5	0.774 ± 0.008	157.4	0.760 ± 0.008	192.9	0.672 ± 0.008
	235.7	0.786 ± 0.010	200.0	0.767 ± 0.009		
	279.9	0.873 ± 0.011				
	335.4	1.013 ± 0.013				
2.502 + 1.509	3.0	0.171 ± 0.001	3.7	0.134 ± 0.001	5.5	0.119 ± 0.001
	6.8	0.319 ± 0.002	7.9	0.284 ± 0.002	13.2	0.249 ± 0.002
	24.3	0.443 ± 0.003	18.5	0.422 ± 0.003	26.5	0.377 ± 0.003
	35.9	0.553 ± 0.004	44.2	0.524 ± 0.004	50.5	0.485 ± 0.004
	77.6	0.617 ± 0.005	69.4	0.598 ± 0.005	75.4	0.550 ± 0.005
	108.9	0.651 ± 0.006	97.1	0.646 ± 0.006	104.4	0.585 ± 0.006
	127.6	0.669 ± 0.007	118.1	0.671 ± 0.006	126.9	0.609 ± 0.006
	160.3	0.679 ± 0.007	136.4	0.723 ± 0.007	157.0	0.634 ± 0.007
	241.1	0.706 ± 0.010	149.0	0.829 ± 0.008		
	251.2	0.797 ± 0.010	180.8	0.856 ± 0.009		

[a]The standard uncertainties (u) associated with the measured quantity are u (T) = 0.1 K and u (P_{CO2}) = 0.5 kPa. α_{CO2} is the CO_2 loading of the solvent in mol of CO_2 per mol of solvent.

$$[H^+] + [2 - MPZH^+] + [R_1H^+] = [HCO_3^-] + 2 \times [CO_3^{2-}] + [OH^-] + [2 - MPZCOO^-] + [R_1COO^-] \quad (5)$$

where, α_{CO2} is the CO_2 loading, and M_1 and M_2 represent the initial [bmim] [Ac] and 2-MPZ molar concentrations, respectively. Furthermore, M_1 indicates the molar concentration of MDEA and $TMSO_2$ for aq (MDEA + 2-MPZ) and aq ($TMSO_2$ + 2-MPZ) systems, respectively.

The systems in eqs 1−5 and Table S2 can be utilized to develop a polynomial equation as a function of $[H^+]$. The equation hence formed for systems under consideration associated with the coefficients can be given as follows:

$$A_2 \times [H^+]^7 + B_2 \times [H^+]^6 + C_2 \times [H^+]^5 + D_2 \times [H^+]^4 + E_2 \times [H^+]^3 + F_2 \times [H^+]^2 + G_2 \times [H^+] + I_2 = 0 \quad (6)$$

where

$$A_2 = K_5 \times K_7 \quad (6.1)$$

$$B_2 = K_5 \times K_7 \times (K_6 + K_4 + M_1 + M_2) \quad (6.2)$$

$$C_2 = K_4 \times K_7 \times \{K_5 \times K_6 + K_2 \times [CO_2] + M_2 \times K_5\} + K_5 \times K_7 \times \{M_1 \times K_6 + M_2 \times K_4 - K_2 \times [CO_2] - K_3\} + K_2 \times K_5 \times K_6 \times [CO_2] \quad (6.3)$$

$$D_2 = K_2 \times K_6 \times [CO_2] \times \{K_4 \times K_7 + K_4 \times K_5 + M_1 \times K_5 - K_5 \times K_7 - M_2 \times K_5\} + K_2 \times K_4 \times K_7 \times [CO_2] \times \{M_2 - K_5 - M_1\} - K_5 \times K_7 \times \{2 \times K_1 \times K_2 \times [CO_2] + K_3 \times K_4 + K_3 \times K_6\} \quad (6.4)$$

$$E_2 = K_2^2 \times [CO_2]^2 \times \{K_4 \times K_6 - K_5 \times K_6 - K_4 \times K_7\} - K_2 \times K_5 \times K_7 \times [CO_2] \times \{K_4 \times K_6 + 2 \times K_1 \times K_4 + 2 \times K_1 \times K_6\} - K_2 \times K_3 \times [CO_2] \times \{K_5 \times K_6 + K_4 \times K_7\} - K_2 \times K_4 \times K_6 \times [CO_2] \times \{K_7 \times M_1 + K_5 \times M_2\} - K_3 \times K_4 \times K_5 \times K_6 \times K_7 \quad (6.5)$$

https://doi.org/10.1021/acsomega.2c02217
ACS Omega 2022, 7, 23611−23623

Table 3. CO_2 Solubility Data in aq ($TMSO_2$ + 2-MPZ) Solution[a]

aq ($TMSO_2$+ 2-MPZ)	T = 303.2 K		T = 313.2 K		T = 323.2 K	
molal (m)	P_{CO2}/kPa	α_{CO2}	P_{CO2}/kPa	α_{CO2}	P_{CO2}/kPa	α_{CO2}
3.501 + 0.509	62.7	0.124 ± 0.003	45.6	0.089 ± 0.002	49.2	0.079 ± 0.002
	128.5	0.133 ± 0.004	123.8	0.097 ± 0.003	114.0	0.084 ± 0.003
	160.7	0.141 ± 0.005	161.8	0.105 ± 0.004	142.4	0.090 ± 0.004
	195.1	0.150 ± 0.006	201.9	0.112 ± 0.005	168.0	0.095 ± 0.004
	252.4	0.156 ± 0.007	257.7	0.117 ± 0.006	178.0	0.128 ± 0.005
	343.9	0.167 ± 0.009	302.3	0.125 ± 0.007	183.8	0.151 ± 0.005
	316.3	0.285 ± 0.009	356.1	0.139 ± 0.008		
	317.6	0.289 ± 0.009				
3.012 + 1.008	4.9	0.167 ± 0.001	9.8	0.126 ± 0.001	21.5	0.144 ± 0.002
	87.5	0.214 ± 0.003	84.3	0.176 ± 0.003	78.7	0.205 ± 0.003
	130.0	0.219 ± 0.004	125.7	0.183 ± 0.004	123.4	0.224 ± 0.004
	165.8	0.222 ± 0.005	159.8	0.191 ± 0.005	171.9	0.232 ± 0.005
	196.5	0.226 ± 0.006	200.2	0.203 ± 0.005	223.3	0.231 ± 0.006
	293.7	0.245 ± 0.008	235.7	0.211 ± 0.006	246.6	0.235 ± 0.006
	303.4	0.259 ± 0.008	299.2	0.239 ± 0.008		
2.500 + 1.509	2.0	0.161 ± 0.001	3.8	0.149 ± 0.001	3.9	0.131 ± 0.001
	36.7	0.281 ± 0.003	38.9	0.262 ± 0.003	18.6	0.249 ± 0.002
	113.8	0.302 ± 0.004	105.8	0.293 ± 0.004	89.4	0.287 ± 0.004
	138.7	0.306 ± 0.005	157.8	0.305 ± 0.005	117.1	0.295 ± 0.004
	167.0	0.312 ± 0.005	187.6	0.313 ± 0.006	147.7	0.295 ± 0.005
	200.3	0.313 ± 0.006	207.2	0.324 ± 0.006	172.1	0.293 ± 0.005
	238.6	0.315 ± 0.007	249.9	0.334 ± 0.007		
	280.6	0.369 ± 0.008				
	316.3	0.399 ± 0.009				

[a]The standard uncertainties (u) associated with the measured quantity are u (T) = 0.1 K and u (P_{CO2}) = 0.5 kPa. α_{CO2} is the CO_2 loading of the solvent in mol of CO_2 per mol of the solvent.

$$F_2 = -K_2^2 \times [CO_2]^2 \times \{K_4 \times K_6 \times (K_5 + K_7) + 2 \times K_1 \times (K_5 \times K_6 + K_4 \times K_7) + K_4 \times K_6 \times (M_1 + M_2)\} - K_2 \times K_4 \times K_6 \times [CO_2] \times \{2 \times K_1 \times K_5 \times K_7 + K_3 \times (K_5 + K_7)\} \quad (6.6)$$

$$G_2 = -K_2^2 \times K_4 \times K_6 \times [CO_2]^2 \times \{K_2 \times [CO_2] + 2 \times K_1 \times K_7 + K_3\} - 2 \times K_1 \times K_2^2 \times K_4 \times K_5 \times K_6 \quad (6.7)$$

$$I_2 = -2 \times K_2^3 \times K_1 \times K_4 \times K_6 \times [CO_2]^3 \quad (6.8)$$

The modified form of the loading equation for the aq ([bmim] [Ac] + 2-MPZ) system is represented as follows:

$$\alpha_{CO_2} = \frac{P_{CO_2}}{(H_{CO_2} \times (M_1 + M_2))}\left[1 + \frac{K_2}{[H^+]} + \frac{K_1 \times K_2}{[H^+]^2} + \frac{M_1 \times K_2 \times K_4}{K_4 \times K_5 \times [H^+] + K_5 \times [H^+]^2 + K_2 \times K_4 \times \left[\frac{P_{CO_2}}{H_{CO_2}}\right]} + \frac{M_2 \times K_2 \times K_6}{K_6 \times K_7 \times [H^+] + K_7 \times [H^+]^2 + K_2 \times K_6 \times \left[\frac{P_{CO_2}}{H_{CO_2}}\right]}\right] \quad (7)$$

α_{CO2} is calculated using eq 7 using the real root of $[H^+]$ obtained from eq 6. In the modified KE model, the equilibrium constants K_1–K_3 and K_8 can be correlated as functions of temperature as given below

$$\ln K = a_i + \frac{b_i}{T} + (c_i \times \ln(T)) \quad (8)$$

where, a_i, bi, and c_i are coefficients of the above equation, and the values of the same are taken from the literature.[54]

The resulting non-linear and linear simultaneous equations are further required to be solved using an optimization algorithm.[38,41] The optimized equilibrium constants K_4, K_5, K_6, K_7, and K_8, which correspond to the deprotonation and carbamate hydrolysis reactions of various reactive species, are estimated as functions of P_{CO2}, T, and solvent concentration (MATLAB17). The solution of eq 6 results in multiple roots of $[H^+]$ but only a single value of $[H^+]$ that belongs in the array of 10^{-12}–10^{-5} kmol. m^{-3} has been used for α_{CO2} estimation. The accuracy of the KE toward prediction of the CO_2 loading is analyzed using % AAD as stated below

$$\text{average absolute deviation: \% AAD} = \frac{100}{N} \times \left(\sum_{i=1}^{N} \frac{|Y^i_{exp} - Y^i_{mod}|}{Y^i_{exp}}\right) \quad (9)$$

where, N, Y^i_{exp}, and Y^i_{mod} indicate the number of data points, the experimental value of α_{CO2}, and the modified KE correlated value of α_{CO2}, respectively.

5. RESULTS AND DISCUSSION

5.1. Influence of Various Reaction Factors on α_{CO2} and Modified Kent–Eisenberg Modeling of Vapor–Liquid Equilibrium Data. The experimental data of CO_2

https://doi.org/10.1021/acsomega.2c02217
ACS Omega 2022, 7, 23611–23623

Table 4. CO_2 Solubility Data in aq ([bmim] [Ac] + 2-MPZ) Solution[a]

aq ([bmim] [Ac]+ 2-MPZ)	T = 303.2 K		T = 313.2 K		T = 323.2 K	
molal (m)	P_{CO2}/kPa	α_{CO2}	P_{CO2}/kPa	α_{CO2}	P_{CO2}/kPa	α_{CO2}
3.507 + 0.509	64.4	0.085 ± 0.003	87.6	0.056 ± 0.003	62.7	0.047 ± 0.002
	114.9	0.105 ± 0.004	121.0	0.086 ± 0.004	98.2	0.072 ± 0.003
	149.9	0.113 ± 0.005	178.5	0.093 ± 0.005	121.1	0.073 ± 0.004
	197.3	0.118 ± 0.006	221.7	0.104 ± 0.007	153.0	0.077 ± 0.005
	235.9	0.125 ± 0.007	254.0	0.122 ± 0.008	180.2	0.082 ± 0.005
	300.2	0.148 ± 0.009	293.3	0.142 ± 0.009	205.5	0.086 ± 0.006
	313.0	0.176 ± 0.010	318.5	0.191 ± 0.010	247.7	0.092 ± 0.007
3.002 + 1.008	22.2	0.144 ± 0.002	35.7	0.113 ± 0.002	23.0	0.107 ± 0.002
	104.8	0.178 ± 0.004	99.1	0.158 ± 0.004	87.6	0.149 ± 0.003
	128.1	0.187 ± 0.005	144.9	0.179 ± 0.005	129.1	0.160 ± 0.004
	163.9	0.191 ± 0.006	192.4	0.187 ± 0.006	176.2	0.169 ± 0.006
	202.8	0.199 ± 0.007	248.7	0.191 ± 0.008	213.7	0.174 ± 0.007
	247.5	0.205 ± 0.008	302.5	0.197 ± 0.009	255.7	0.183 ± 0.008
	269.8	0.288 ± 0.009	326.1	0.268 ± 0.010		
	317.4	0.254 ± 0.010	370.1	0.299 ± 0.011		
2.510 + 1.509	3.5	0.183 ± 0.002	4.6	0.152 ± 0.002	5.0	0.122 ± 0.001
	68.1	0.273 ± 0.004	83.7	0.219 ± 0.004	59.7	0.194 ± 0.003
	126.2	0.283 ± 0.005	104.2	0.253 ± 0.004	98.1	0.225 ± 0.004
	162.7	0.291 ± 0.006	125.4	0.269 ± 0.005	132.7	0.244 ± 0.005
	208.2	0.297 ± 0.007	156.4	0.276 ± 0.006	148.9	0.275 ± 0.005
	243.3	0.303 ± 0.008	193.9	0.284 ± 0.007	157.4	0.328 ± 0.006
	262.2	0.372 ± 0.009	222.8	0.356 ± 0.008		
	301.3	0.363 ± 0.010				

[a]The standard uncertainties (u) associated with the measured quantity are u (T) = 0.1 K and u (P_{CO2}) = 0.5 kPa. α_{CO2} is the CO_2 loading of the solvent in mol of CO_2 per mol of solvent.

Table 5. Coefficients of Equilibrium Constants Estimated in the Present Work[a]

system	aq (MDEA + 2-MPZ)		aq ([bmim] [Ac] + 2-MPZ)				aq ($TMSO_2$ + 2-MPZ)	
K_i/kmol.m^{-3}	K_4	K_5	K_4	K_5	K_6	K_7	K_4	K_5
G	-3.216×10^{-8}	4.174×10^{5}	-9.782×10^{-9}	-2.485×10^{3}	-9.795×10^{-9}	-2.513×10^{3}	2.586×10^{-5}	-5.439×10^{4}
H	-1.261×10^{-9}	9.951×10	-4.436×10^{-9}	-4.826×10^{3}	-4.436×10^{-9}	-4.840×10^{3}	-2.399×10^{-5}	-5.814×10
K	1.024×10^{-10}	5.933×10	6.745×10^{-11}	-5.974×10	6.740×10^{-11}	-5.990×10	2.492×10^{-8}	5.817×10^{3}
L	6.755×10^{-12}	-3.978	-2.327×10^{-11}	-1.627×10^{3}	-2.328×10^{-11}	-1.619×10^{3}	-7.333×10^{-9}	-4.496×10^{2}
N	2.168×10^{-14}	-5.624	2.612×10^{-13}	5.822	2.597×10^{-13}	5.830	-5.254×10^{-11}	-1.541×10
P	-7.678×10^{-13}	-3.410×10^{-2}	1.131×10^{-10}	-5.177×10^{-2}	1.132×10^{-10}	-5.164×10^{-2}	9.969×10^{-10}	-2.062×10
Q	2.728×10^{-14}	1.885×10^{-2}	1.555×10^{-24}	9.442×10^{2}	1.563×10^{-24}	9.453×10^{2}	-3.294×10^{-13}	1.014×10^{3}
R		-1.799×10^{-4}		-1.359×10^{-3}		-1.388×10^{-3}		-7.680×10^{-2}
% AAD	7.53			22.49			31.94	

[a]The competency of the modified KE model for prediction of CO_2 solubility is also presented in terms of residual plots for the aq (MDEA + 2-MPZ) system in Figure 3.

partial pressure with respect to each loading along with the associated uncertainty are presented in Tables 2−4. The standardization of the conceived methodology for the present work has been previously reported by our research group.[38,40,41,67] The maximum evaluated uncertainty of CO_2 loading is 0.013.

The CO_2 solubility data have been associated using the modified KE model. The results of correlation were used to evaluate the coefficients of the equilibrium constants K_4, K_5, K_6, *and* K_7 using non-linear regression analysis. A non-linear optimization method with the objective function as eq 9 was employed to reduce the imprecision between the experimental and predicted values. The evaluated equilibrium constants (K_4, K_5, K_6, and K_7) in terms of concentration of solvents, T, and P_{CO2} can be expressed as follows:

$$K_4(or/K_6) = g + (h \times M) + (k \times T) + (l \times M \times T) + (n \times T^2) + (p \times P_{CO_2}) + (q \times P_{CO_2}^2) \quad (10)$$

$$K_5(or/K_7) = g + (h \times M) + (k \times T) + (l \times M^2) + (n \times M \times T) + (p \times T^2) + (q \times P_{CO2}) + (r \times P_{CO_2}^2) \quad (11)$$

where g, h, k, l, n, p, q, and r are the coefficients associated with the equilibrium constants and are found by optimization. The calculated values of equilibrium constants are given in Table 5. The equilibrium constants obtained through the KE model were in turn used to predict α_{CO2}. The calculated % AAD for aq (MDEA + 2-MPZ), aq ([bmim] [Ac] + 2-MPZ), and aq

https://doi.org/10.1021/acsomega.2c02217
ACS Omega 2022, 7, 23611−23623

($TMSO_2$ + 2-MPZ) systems is 7.53, 22.49, and 31.94, respectively.

CO_2 solubility is seen to decline with the increase in temperature for all systems under study (Tables 2−4). This decrease in α_{CO2} is due to the exothermic nature of reaction in proposed solvents and CO_2. With the increase in the 2-MPZ activator concentration in the blend keeping the overall concentration of the solvents unchanged, an increase in CO_2 solubility is also perceived in the aqueous blends. Additionally, with intensification in P_{CO2}, it is observed that α_{CO2} increases since an increase in system pressure results in the growth in kinetic energy associated with the gas molecules. This further leads to the improvement of the rate of diffusion up to a positive maximum limit. The number of collisions between gas molecules and the liquid surface increases when P_{CO2} is increased. This subsequently results in higher CO_2 loading. However, after this limiting value of P_{CO2}, there is no remarkable increase in CO_2 loading. The experimental and modeled α_{CO2} values of aq (3.509 *m* MDEA + 0.509 *m* 2-MPZ) and aq (3.002 *m* [bmim] [Ac] + 1.008 *m* 2-MPZ) are studied as a function of temperature (Figure 4a,b). The results

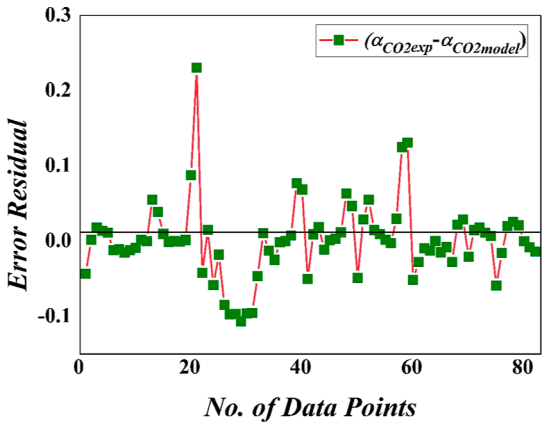

Figure 3. Residual plot of the aq (MDEA + 2-MPZ) system.

offer a decent covenant of the measured experimental data with the modeled α_{CO2}. A contour analysis of the aq ($TMSO_2$ + 2-MPZ) system indicates that the system absorbed more CO_2 at low temperatures and high pressures (Figure 4c).

The increase in concentration of 2-MPZ from 0.509 to 1.509 *m* in the aqueous solution of [bmim] [Ac] results in an increase in α_{CO2} at all temperatures, viz., (303.2, 313.2, and 323.2 K) (Figure 5a). It can be concluded that a 1.509 *m* concentration of 2-MPZ is highly appreciable and provides far better CO_2 solubility in comparison to the 0.509 *m* concentration of 2-MPZ in a blended system. The studies on the effect of the base solvent with the activator (2-MPZ) indicate that blends of MDEA with 2-MPZ provide superior α_{CO2} in comparison to [bmim] [Ac] or $TMSO_2$ at the same solvent concentration and temperature (Figure 5b). MDEA, being a tertiary amine, has an amino group that reacts chemically with CO_2, providing chemical absorption. Hence, in the aq (MDEA + 2-MPZ) solvent mixture, the amino groups responsible for reacting with CO_2 are higher when compared to aq ([bmim] [Ac] + 2-MPZ) and aq ($TMSO_2$ + 2-MPZ) solvent blends. This can be correlated with the fact that both ionic liquids and physical solvents react only physically majorly, which is quite low at a low P_{CO2}, whereas MDEA majorly contributes through chemical absorption. Along with

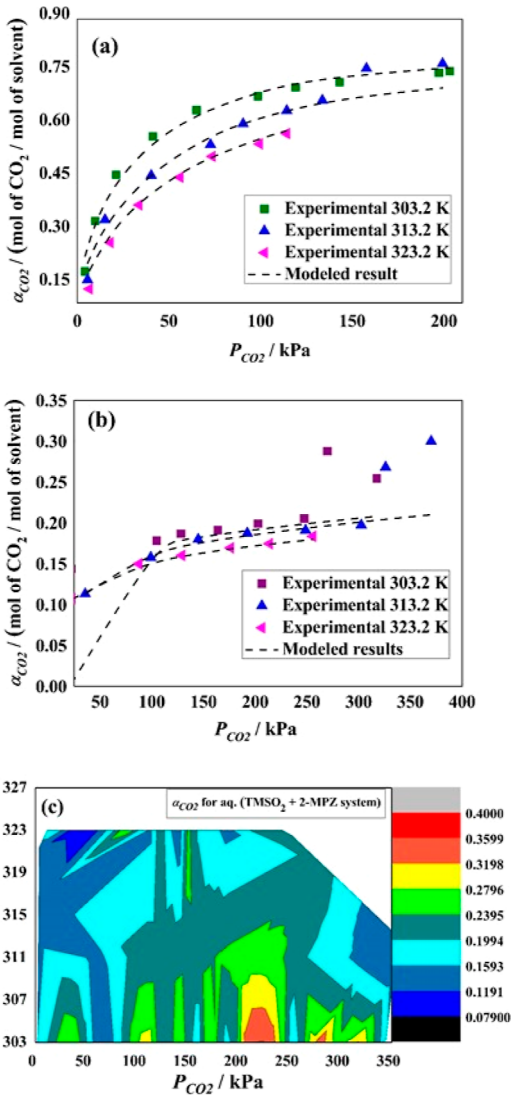

Figure 4. CO_2 solubility in the aqueous blends of (a) aq (3.509 *m* MDEA + 0.509 *m* 2-MPZ) and (b) aq (3.002 *m* [bmim] [Ac] + 1.008 *m* 2-MPZ) as a function of temperature and (c) aq ($TMSO_2$ + 2-MPZ) as functions of *T* and P_{CO2} ("*m*" signifies mol.kg^{-1}).

this, the ionic liquid blended with 2-MPZ shows better performance than that blended with $TMSO_2$. The total CO_2 solubility offered by any solvent is the sum effect of physical and chemical absorption. The former depends on the structure and is due to van der Waals forces of attraction, whereas the latter is due to the number of functional groups (majorly amino groups) available for chemical reaction. For the aq (MDEA + 2-MPZ) system, the amino groups are present in both MDEA and 2-MPZ, and CO_2 solubility depends on both the solvents. The studied concentrations are (3.509 *m* MDEA + 0.509 *m* 2-MPZ), (3.017 *m* MDEA + 1.008 *m* 2-MPZ) and (2.502 MDEA *m* + 1.509 *m* 2-MPZ), where simultaneously, the activator 2-MPZ is increased and MDEA is decreased. Hence, it can be concluded that for the concentration of (2.502 *m* MDEA + 1.509 *m* 2-MPZ), the total number of amino groups present in the solution available to react with CO_2 is less compared to the (3.017 *m* MDEA + 1.008 *m* 2-MPZ) system. This behavior is also justified because in [bmim] [Ac] and $TMSO_2$ systems this does not occur. Both [bmim] [Ac] and $TMSO_2$ offer major physical absorption, as

https://doi.org/10.1021/acsomega.2c02217
ACS Omega 2022, 7, 23611−23623

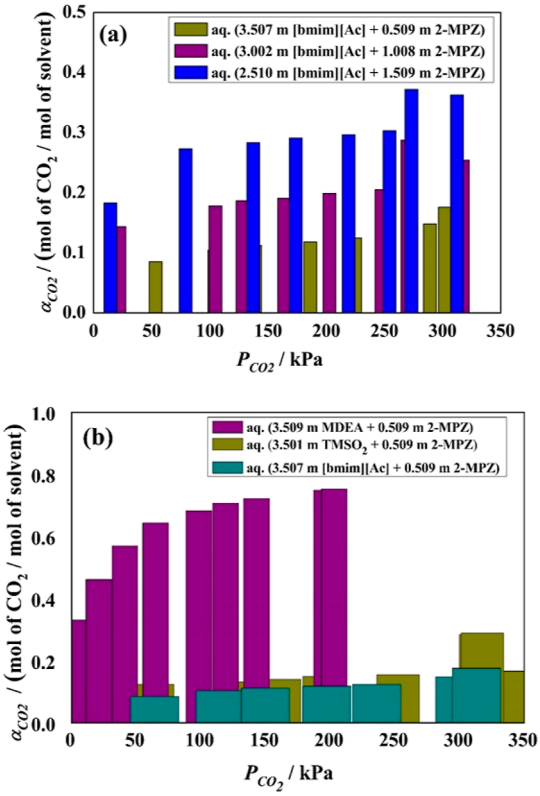

Figure 5. (a) Effect on CO_2 solubility with addition of 2-MPZ in aq [bmim] [Ac] at 303.2 K. (b) CO_2 solubility comparison in $TMSO_2$, MDEA, and [bmim] [Ac] added with 2-MPZ at 303.2 K ("*m*" signifies "mol/kg").

they are an ionic liquid and a physical solvent, respectively, and chemical absorption is majorly contributed through the 2-MPZ activator. Furthermore, quantifying the CO_2 solubility data indicates that for the aq (MDEA + 2-MPZ) system at 313.2 K and 200 kPa, the increase in α_{CO2} observed is only 1.059% with an increase in 2-MPZ concentration from 0.509 to 1.008 *m*. However, the subsequent increase in the concentration of 2-MPZ from 0.509 to 1.509 *m* results in an increase in α_{CO2} by 16.13%. Hence, it can be concluded that the CO_2 solubility is in the order of MDEA > [bmim] [Ac] > $TMSO_2$ with the same activator concentration (2-MPZ) in all blended solutions.

5.2. Liquid Phase Speciation Profile and pH. The equilibrium concentrations of different species in the solvent phase are further predicted as a function of α_{CO2} using the modified KE model. The concentration profiles of diverse species for CO_2-loaded (3.509 *m* MDEA + 0.509 *m* 2-MPZ) at 303.2 K and (3.002 *m* [bmim] [Ac] + 1.008 *m* 2-MPZ) at 313.2 K have been established through the results of $[H^+]$ obtained by the KE model (Figure S1a,b). As indicated, there is a sharp decrease in the concentrations of 2-MPZ as a function of α_{CO2}, indicating it to be a limiting reactant for CO_2 solubility reaction. Also, it is evident from the speciation that HCO_3^- and carbamate, corresponding to an ionic liquid and an amine, are associated to be the major reaction products. The estimation of the pH of the reactants, products, as well as intermediate species, is one of the important design parameters for absorption and stripping tower systems. The reaction products of the CO_2 solubility systems are usually in the pH range of (7−12).[68] In the current work, the modified KE model is further used to evaluate the pH of the blended solvent systems as a function of α_{CO2}. For the aq (2.500 *m* $TMSO_2$ + 1.509 *m* 2-MPZ) system, the maximum pH of 8.8 was observed at a low temperature of 303.2 K (Figure S1c). With the increase in *T* and α_{CO2}, the pH was observed to decrease inevitably because of the fact that there were more H^+ ions in the systems in comparison to OH^- ions at lower temperatures.

5.3. CO_2 Cyclic Capacity. The solvent transmission rate in the absorption−regeneration route is often taken as the performance indicator, which is directly a function of CO_2 cyclic capacity.[69] In the present work, the CO_2 cyclic capacity has been estimated for the aq (MDEA + 2-MPZ) system using eq 12

$$\text{capacity}\left(\frac{\text{moles}CO_2}{\text{kgsolvent}}\right) = (\alpha_{PCO2,rich} - \alpha_{PCO2,lean}) \times [\text{MDEA}/2 - \text{MPZ}] \left(\frac{\text{mole}(\text{MDEA}/2 - \text{MPZ})}{\text{kgsolvent}}\right) \quad (12)$$

where, $\alpha_{PCO2,\ rich}$ is evaluated at 20, 30, and 40 kPa, and $\alpha_{PCO2,\ lean}$ is calculated at 5 kPa. The CO_2 cyclic capacity of the system has been evaluated at 303.2 K with respect to MDEA and 2-MPZ concentration (Figure S2a,b). The total CO_2 cyclic capacity of the ≈ 4 *m* (MDEA + 2-MPZ) system is observed to be 1.039. However, with respect to MDEA and 2-MPZ concentrations, the maximum of the parameters was observed to be 0.908 and 0.307 at 40 kPa, the highest partial pressure of the system. It indicates that owing to the much larger concentration of MDEA in comparison to 2-MPZ, the CO_2 cyclic capacity depends on MDEA rather than on 2-MPZ. The dependency of CO_2 cyclic capacity on temperature (Figure S2c) concludes that with the increase in temperature, the CO_2 cyclic capacity also tends to decrease, similar to α_{CO2}. Additionally, the CO_2 cyclic capacity estimated for the ≈ 4 *m* (MDEA + 2-MPZ) system is found to be approximately 51.59% higher than 30 wt % MEA solution (∼7 *m*),[70] hence indicating that the utilization of the proposed solvent blends will require a smaller equipment size for absorption and less recirculation of the fresh solvent.

5.4. Heat of Absorption in the aq (MDEA + 2-MPZ) Solvent. CO_2 absorption in any solvent, whether amines or ionic liquids, results in generation of heat due to the usual exothermic nature of the reactions involved. This indicates that if the heat of absorption is higher, it will result in a high energy requirement during regeneration. Hence, the energy requirements for any solvent desorption process are dictated by the heat of CO_2 absorption. The latter can either be measured experimentally using instruments such as a reaction calorimeter or can be evaluated from VLE data using the Gibbs−Helmholtz equation.[71] The equation is presented as follows:

$$\frac{d(\ln P_{CO2})}{d\left(\frac{1}{T}\right)} = \frac{\Delta H_a}{R} \quad (13)$$

The heat of absorption in aq (3.509 *m* MDEA + 0.509 *m* 2-MPZ) is obtained by eq 13 using the slope of the plot of $\ln(P_{CO2})$ versus $(1/T)$. As revealed in Figure S2d, plots were made with α_{CO2} = 0.37, 0.47, and 0.57, corresponding to which the obtained slopes were −4783.69, −4675.13, and −4873.65, respectively. The obtained heat of absorption is presented in Table 6. In comparison to activated aq MEA or DEA systems, that is, primary or secondary amines, tertiary amines exhibit a

https://doi.org/10.1021/acsomega.2c02217
ACS Omega 2022, 7, 23611−23623

Table 6. Heat of Absorption in aq (3.509 *m* MDEA + 0.509 *m* 2-MPZ) at Various Compositions within the Temperature Range of 303.2−333.2 K

α_{CO2}	ΔHa (kJ/mol)
0.37	−39.77
0.47	−38.87
0.57	−40.52

lower heat of absorption. This is owing to the reason that primary amines form carbamate and dicarbamate, which result in high heat of absorption, whereas bicarbonate formation, which is one of the principal reactions occurring in tertiary amine systems, is an endothermic reaction.[72] Comparable interpretations have also been reported in the literature.[73−75] The uncertainty associated with pH and heat of absorption is found using the equation given in serial number 6 in Table S1.[76] Both the variables are found to depend on four major parameters of the system, that is, temperature, CO_2 partial pressure, CO_2 loading, and concentration of the solvent. Hence, the uncertainty associated with each of these variables is considered in order to evaluate the uncertainty in pH and heat of absorption calculations. The maximum uncertainty associated with pH and heat of absorption was found to be: aq (MDEA + 2-MPZ): 0.1126, aq ([bmim] [Ac] + 2-MPZ): 0.1123, and aq ($TMSO_2$ + 2-MPZ): 0.1122.

5.5. Comparison with Literature CO_2 Solubility. An assessment of the studied solvents is done with the available literature. However, due to the lack of literature in the studied range of composition, the nearest available literature was considered. CO_2 solubility in the blend of aq (3.017 *m* MDEA + 1.008 *m* 2-MPZ) solution is quite competitive to literature available data (Figure 6).[10,18,77] In addition, a comparison of

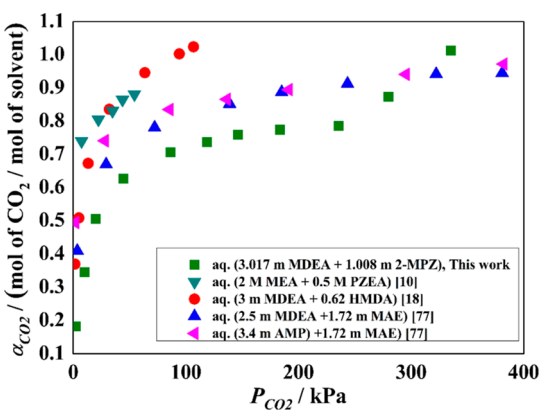

Figure 6. Comparison of CO_2 solubility in aq (3.017 *m* MDEA + 1.008 *m* 2-MPZ) with the literature at 303.2 K ("*m*" signifies "mol/kg":).

aq (3.501 *m* $TMSO_2$ + 0.509 *m* 2-MPZ) with a near-aqueous composition of 0.0999 mol fractions of $TMSO_2$ indicates that the former provides a maximum CO_2 solubility of 0.0191 mol fraction at 317.57 kPa. On the other hand, aq $TMSO_2$ provides a CO_2 solubility of 0.0106 mol fraction at 1.108 MPa and at 303.2 K. Hence, it can be concluded that with the addition of 0.509 *m* 2-MPZ to nearly the same composition of $TMSO_2$, the newly developed blend outperforms the aqueous blend of $TMSO_2$.

6. CONCLUSIONS

CO_2 solubility in aq MDEA, $TMSO_2$, and [bmim] [Ac] enhanced by the PZ-based amine activator, viz., 2-MPZ was studied over inclusive variations in experimental conditions. Qualitative analysis through FTIR and ^{13}C NMR of the unloaded and loaded solvents indicated carbamate formation by 2-MPZ reacting with CO_2. The results evidently specify that CO_2 solubility increases with respect to an increase in both P_{CO2} and concentrations of activators in solvent blends. A modified KE model was developed to correlate the CO_2 solubility data. Results indicated that an increase in 2-MPZ in blends of aq. MDEA, $TMSO_2$, or [bmim] [Ac] improved the CO_2 solubility tremendously. The optimized equilibrium constants associated with various reactions as functions of P_{CO2}, solvent concentration, and *T* of absorption have been estimated using regression analysis. The speciation and pH data as a function of α_{CO2} have been estimated by means of the modified KE model. The CO_2 cyclic capacity and low heat of absorption of the aq (MDEA + 2-MPZ) solvent indicated it to be a prospective solvent for CO_2 capture. In addition, an assessment of CO_2 solubility data of solvent blends with the literature reveals that the considered solvents have good potential for post-combustion CO_2 capture applications.

■ ASSOCIATED CONTENT

Supporting Information

The Supporting Information is available free of charge at https://pubs.acs.org/doi/10.1021/acsomega.2c02217.

Table S1 Details of equations for calculation of α_{CO2} and associated uncertainty; Table S2 Reaction, reaction mechanism, and equilibrium constants associated with reactions in the system; Figure S1 Modified KE model-predicted equilibrium liquid phase concentration of various species in CO_2-loaded aq (3.509 *m* MDEA + 0.509 *m* 2-MPZ) at *T* = 303.2 K and aq (3.002 *m* [bmim] [Ac] + 1.008 *m* 2-MPZ) at *T* = 313.2 K and pH as a function of CO_2 loading in aq (2.500 *m* $TMSO_2$ + 1.509 *m* 2-MPZ); CO_2 cyclic capacity of the aq (MDEA + 2-MPZ) system at 303.2 K with $P_{CO2,\ lean}$ = 5 kPa as functions of MDEA concentration and 2-MPZ concentration; Figure S2 CO_2 cyclic capacity of the aq (3.509 *m* MDEA + 0.509 *m* 2-MPZ) system with $P_{CO2,\ lean}$=5 kPa as a function of temperature; and plot of $\ln(P_{CO2})$ with $1/T$ for calculation of heat of absorption for the aq (MDEA + 2-MPZ) system (PDF)

■ AUTHOR INFORMATION

Corresponding Author

Bishnupada Mandal − *Department of Chemical Engineering, Separation Science Laboratory, Indian Institute of Technology Guwahati, Guwahati 781039, India;* orcid.org/0000-0003-1971-3804; Phone: +91-361-2582256; Email: bpmandal@iitg.ac.in; Fax: +91-79-2582290

Authors

Sweta C. Balchandani − *Department of Chemical Engineering, Separation Science Laboratory, Indian Institute of Technology Guwahati, Guwahati 781039, India; CO_2 Research Group, Department of Chemical Engineering, School of Technology, Pandit Deendayal Energy University, Gandhinagar 382007, India*

https://doi.org/10.1021/acsomega.2c02217
ACS Omega 2022, 7, 23611−23623

Swapnil Dharaskar − *CO_2 Research Group, Department of Chemical Engineering, School of Technology, Pandit Deendayal Energy University, Gandhinagar 382007, India*

Complete contact information is available at:
https://pubs.acs.org/10.1021/acsomega.2c02217

Notes

The authors declare no competing financial interest.

■ REFERENCES

(1) Astaria, G.; Savage, D. W.; Bisio, A. *Gas treating with chemical solvents*; John Wiley and Sons: New York, 1983.

(2) Bishnoi, S.; Rochelle, G. T. Absorption of carbon Dioxide in aqueous piperazine/methyldiethanolamine. *AIChE J.* **2002**, *48*, 2788−2799.

(3) Nagao, Y.; Hayakawa, A.; Suzuki, H.; Mitsuoka, S.; lwaki, T.; Mimura, T.; Suda, T. Comparative study of various amines for the eversible absorption capacity of carbon dioxide. *Stud. Surf. Sci. Catal.* **1998**, *114*, 669−672.

(4) Tiwari, S. C.; Pant, K. K.; Upadhyayula, S. Efficient CO2 absorption in aqueous dual functionalized cyclic ionic liquids. *J. CO2 Util.* **2021**, *45*, 101416.

(5) Bi, Y.; Hu, Z.; Lin, X.; Ahmad, N.; Xu, J.; Xu, X. Efficient CO_2 capture by a novel deep eutectic solvent through facile, one pot synthesis with low energy consumption and feasible regeneration. *Sci. Total Environ.* **2020**, *705*, 135798.

(6) Mason, J. W.; Dodge, B. F. Equilibrium absorption of carbon dioxide by solutions of the ethanolamines. *Trans. Institutions Chem. Eng.* **1936**, *32*, 27−48.

(7) Mamun, S.; Nilsen, R.; Svendsen, H. F. Solubility of carbon dioxide in 30 mass % monoethanolamine and 50 mass % methyldiethanolamine solutions. *J. Chem. Eng. Data* **2005**, *50*, 630−634.

(8) Kennard, M. L.; Meisen, A. Solubility of carbon dioxide in aqueous diethanolamine solutions at elevated temperatures and pressures. *J. Chem. Eng. Data* **1984**, *29*, 309−312.

(9) Teng, T. T.; Mather, A. E. Solubility of H_2S, CO_2, and their mixtures in an AMP solution. *Can. J. Chem. Eng.* **1989**, *67*, 846−850.

(10) Ramazani, R.; Mazinani, S.; Hafizi, A.; Jahanmiri, A. Equilibrium solubility of carbon dioxide in aqueous blend of monoethanolamine (MEA) and 2-1-piperazinyl-ethlamine (PZEA) solutions: Experimental and optimization study. *Process Saf. Environ. Prot.* **2015**, *98*, 325−332.

(11) Tong, D.; Maitland, G. C.; Trusler, M. J. P.; Fennell, P. S. Solubility of carbon dioxide in aqueous blends of 2-amino-2-methyl-1-propanol and piperazine. *Chem. Eng. Sci.* **2013**, *101*, 851−864.

(12) Dash, S. K.; Bandyopadhyay, S. S. Studies on the effect of addition of piperazine and sulfolane into aqueous solution of N-methyldiethanolamine for CO_2 capture and VLE modelling using e-NRTL equation. *Int. J. Greenh. Gas Control* **2016**, *44*, 227−237.

(13) Khodadadi, M. J.; Riahi, S.; Abbasi, M. Experimental modeling of the solubility of carbon dioxide in aqueous solution of monoethanolamine + 1, 3-diaminopropane. *J. Mol. Liq.* **2019**, *281*, 415−422.

(14) Kim, Y. E.; Choi, J. H.; Nam, S. C.; Yoon, Y. I. CO_2 absorption capacity using aqueous potassium carbonate with 2-methylpiperazine and piperazine. *J. Ind. Eng. Chem.* **2012**, *18*, 105−110.

(15) Das, B.; Deogam, B.; Mandal, B. Experimental and theoretical studies on efficient carbon dioxide capture using novel bis (3-aminopropyl) amine (APA) −activated aqueous 2-amino-2-methyl-1-propanol (AMP) solutions. *RSC Adv.* **2017**, *7*, 21518−21530.

(16) Das, B.; Deogam, B.; Mandal, B. Absorption of CO_2 into novel aqueous bis (3-aminopropyl) amine and enhancement of CO_2 absorption into its blends with N-methyldiethanolamine. *Int. J. Greenh. Gas Control* **2017**, *60*, 172−185.

(17) Hafizi, A.; Mokari, M. H.; Khalifeh, R.; Farsi, M.; Rahimpour, M. R. Improving the CO_2 solubility in aqueous mixture of MDEA and different polyamine promoters: The effects of primary and secondary functional groups. *J. Mol. Liq.* **2019**, *297*, 111803.

(18) Mondal, B. K.; Bandyopadhyay, S. S.; Samanta, A. N. Equilibrium solubility measurement and Kent-Eisenberg modeling of CO_2 absorption in aqueous mixture of N-methyldiethanolamine and hexamethylenediamine. *Greenhouse Gases: Sci. Technol.* **2016**, *7*, 202−214.

(19) Ramezani, R.; Felice, R. D. Experimental study of CO_2 absorption in different blend solutions as solvent for CO_2 capture. *Int. J. Chem. Biomol. Eng.* **2017**, *11*, 5−10.

(20) Sherman, B.; Frailie, P. T.; Li, L.; Salta, N.; Rochelle, G. T. Thermodynamic and kinetic modeling of piperazine/2-methylpiperazine. *Energy Procedia* **2014**, *63*, 1243−1255.

(21) Chen, X.; Rochelle, G. T. Modeling of CO_2 absorption kinetics in aqueous 2-methylpiperazine. *Ind. Eng. Chem. Res.* **2013**, *52*, 4239−4248.

(22) Chen, X.; Rochelle, G. T. Thermodynamics of CO_2 / 2-methylpiperazine/ water. *Ind. Eng. Chem. Res.* **2013**, *52*, 4229−4238.

(23) Sherman, B.; Chen, X.; Nguyen, T.; Xu, Q.; Rafique, H.; Freeman, S. A.; Voice, A. K.; Rochelle, G. T. Carbon capture with 4 m piperazine/4 m 2-methylpiperazine. *Energy Procedia* **2013**, *37*, 436−447.

(24) Yuan, Y.; Sherman, B.; Rochelle, G. T. Effects of viscosity on CO_2 absorption in aqueous piperazine / 2-methylpiperazine. *Energy Procedia* **2017**, *114*, 2103−2120.

(25) Murrieta-Guevara, F.; Romero-Martinez, A.; Trejo, A. Solubilities of carbon dioxide and hydrogen sulphide in propylene carbonate, N- methylpyrrolidone and sulfolane. *Fluid Phase Equilib.* **1988**, *44*, 105−115.

(26) Shokouhi, M.; Jalili, A. H.; Zoghi, A. T.; Sadeghzadeh Ahari, J. Carbon dioxide solubility in aqueous sulfolane solution. *J. Chem. Thermodyn.* **2019**, *132*, 62−72.

(27) Jalili, A. H.; Shokouhi, M.; Samani, F.; Hosseini-Jenab, M. Measuring the solubility of CO_2 and H_2S in sulfolane and the density and viscosity of saturated liquid binary mixtures of (sulfolane + CO_2) and (sulfolane + H_2S). *J. Chem. Thermodyn.* **2015**, *85*, 13−25.

(28) Jou, F.-Y.; Mather, A. E. Solubility of carbon dioxide in an aqueous mixture of methyldiethanolamine and N-methylpyrrolidone at elevated pressures. *Fluid Phase Equilib.* **2005**, *228-229*, 465−469.

(29) Zong, L.; Chen, C.-C. Thermodynamic modeling of CO_2 and H_2S solubilities in aqueous DIPA solution, aqueous sulfolane-DIPA solution, and aqueous sulfolane-MDEA solution with electrolyte NRTL model. *Fluid Phase Equilib.* **2011**, *306*, 190−203.

(30) Shirazizadeh, H. A.; Haghtalab, A. Simultaneous solubility measurement of (ethyl mercaptans + carbon dioxide) into the aqueous solutions of (N-methyl diethanolamine + sulfolane + water). *J. Chem. Thermodyn.* **2019**, *133*, 111−122.

(31) Wang, L.; Yu, S.; Li, Q.; Zhang, Y.; An, S.; Zhang, S. Performance of sulfolane / DETA hybrids for CO_2 absorption: phase splitting behaviour, kinetics and thermodynamics. *Appl. Energy* **2018**, *228*, 568−576.

(32) Luo, W.; Guo, D.; Zheng, J.; Gao, S.; Chen, J. CO_2 absorption using biphasic solvent: blends of diethylenetriamine, sulfolane, and water. *Int. J. Greenh. Gas Control* **2016**, *53*, 141−148.

(33) Lu, J.-G.; Lu, Z.-Y.; Chen, Y.; Wang, J.-T.; Gao, L.; Gao, X.; Tang, Y.-Q.; Liu, D.-G. CO_2 absorption into aqueous blends of ionic liquid and amine in a membrane contactor. *Sep. Purif. Technol.* **2015**, *150*, 278−285.

(34) Krupiczka, R.; Rotkegel, A.; Ziobrowski, Z. Comparative study of CO_2 absorption in packed column using imidazolium based ionic liquids and MEA solution. *Sep. Purif. Technol.* **2015**, *149*, 228−236.

(35) Bogolitsyn, K. G.; Skrebets, T. E.; Makhova, T. A. Physiochemical properties of 1-butyl-3-methylimidazolium acetate. *Russ. J. Gen. Chem.* **2009**, *79*, 125−128.

(36) Umecky, T.; Abe, M.; Takamuku, T.; Makino, T.; Kanakubo, M. CO_2 absorption features of 1-ethyl-3-methylimidazolium ionic liquids with 2, 4-pentanedionate and its fluorine derivatives. *J. CO_2 Util.* **2019**, *31*, 75−84.

(37) Safarov, J.; Geppert-Rybczyńska, M.; Kul, I.; Hassel, E. Thermophysical properties of 1-butyl-3-methylimidazolium acetate over a wide range of temperatures and pressures. *Fluid Phase Equilib.* **2014**, *383*, 144−155.
(38) Balchandani, S.; Mandal, B.; Dharaskar, S. Measurements and modeling of vapor liquid equilibrium of CO_2 in amine activated imidazolium ionic liquid solvents. *Fluid Phase Equilib.* **2020**, *521*, 112643.
(39) Balchandani, S.; Singh, R. COSMO-RS analysis of CO_2 solubility in N-methyldiethanolamine, sulfolane, and 1-butyl-3-methyl-imidazolium acetate activated by 2-methylpiperazine for post combustion carbon capture. *ACS Omega* **2021**, *6*, 747−761.
(40) Balchandani, S. C.; Mandal, B.; Dharaskar, S. Stimulation of CO_2 solubility in reversible ionic liquids activated by novel 1-(2-aminoethyl piperazine) and bis (3-aminopropyl amine). *Sep. Purif. Technol.* **2021**, *262*, 118260.
(41) Dey, A.; Dash, S. K.; Mandal, B. Equilibrium CO_2 solubility and thermophysical properties of aqueous blends of 1-(2-aminoethyl) piperazine and N-methyldiethanolamine. *Fluid Phase Equilib.* **2018**, *463*, 91−105.
(42) Ahmady, A.; Hashim, M. A.; Aroua, M. K. Absorption of carbon dioxide in the aqueous mixtures of methyldiethanolamine with three types of imidazolium based ionic liquids. *Fluid Phase Equilib.* **2011**, *309*, 76−82.
(43) Mirarab, M.; Sharifi, M.; Ghayyem, M. A.; Mirarab, F. Prediction of solubility of CO_2 in ethanol-[emim] [Tf_2N] ionic liquid mixtures using artificial neural networks based on genetic algorithm. *Fluid Phase Equilib.* **2014**, *371*, 6−14.
(44) Najafloo, A.; Zoghi, A. T.; Feyzi, F. Measuring solubility of carbon dioxide in aqueous blends of N-methyldiethanolamine and 2-((2-aminoethyl) amino) ethanol at low CO_2 loadings and modelling by electrolyte SAFT-HR EoS. *J. Chem. Thermodyn.* **2015**, *82*, 143−155.
(45) Sema, T.; Naami, A.; Idem, R.; Tontiwachwuthikul, P. Correlations for equilibrium solubility of carbon dioxide in aqueous 4-(diethylamino)-2-butanol solution. *Ind. Eng. Chem. Res.* **2011**, *50*, 14008−14015.
(46) Agarwal, N. K.; Mondal, B. K.; Samanta, A. N. Measurement of vapor -liquid equilibrium and e-NRTL model development of CO_2 absorption in aqueous dipropylenetriamine. *Environ. Sci. Pollut. Res.* **2021**, *28*, 19285−19297.
(47) Kim, Y. S.; Choi, W. Y.; Jang, J. H.; Yoo, K.-P.; Lee, C. S. Solubility measurement and prediction of carbon dioxide in ionic liquid. *Fluid Phase Equilib.* **2005**, *228-229*, 439−445.
(48) Na, S.; Hwang, S. J.; Kim, H.; Baek, I.-H.; Lee, K. S. Modeling of CO_2 solubility of an aqueous polyamine solvent for CO_2 capture. *Chem. Eng. Sci.* **2019**, *204*, 140−150.
(49) Voice, A. K.; Vevelstad, S. J.; Chen, X.; Nguyen, T.; Rochelle, G. T. Aqueous 3-(methylamino) propylamine for CO2 capture. *Int. J. Greenh. Gas Control* **2013**, *15*, 70−77.
(50) Yuan, Y.; Rochelle, G. T. CO_2 absorption rate and capacity of semi-aqueous piperazine for CO_2 capture. *Int. J. Greenh. Gas Control* **2019**, *85*, 182−186.
(51) Pinto, A. M.; Rodríguez, H.; Arce, A.; Soto, A. Carbon dioxide absorption in the ionic liquid 1-ethylpyridinium ethylsulphate and its mixture with another ionic liquid. *Int. J. Greenh. Gas Control* **2013**, *18*, 296−304.
(52) Watanabe, M.; Kodama, D.; Makino, T.; Kanakubo, M. CO_2 absorption properties of imidazolium based ionic liquids using a magnetic suspension balance. *Fluid Phase Equilib.* **2016**, *420*, 44−49.
(53) dos Santos, P. F.; André, L.; Ducousso, M.; Contamine, F.; Cézac, P. Experimental measurement of CO_2 solubility in aqueous Na_2SO_4 solution at temperatures between 303.15 and 423.15 K and Pressures upto 20 MPa. *J. Chem. Eng. Data* **2020**, *65*, 3230−3239.
(54) Mondal, B. K.; Bandyopadhyay, S. S.; Samanta, A. N. Vapor-liquid equilibrium measurement and ENRTL modeling of CO_2 absorption in aqueous hexamethylenediamine. *Fluid Phase Equilib.* **2015**, *402*, 102−112.
(55) Böttinger, W.; Maiwald, M.; Hasse, H. Online NMR spectroscopic study of species distribution in MEA-H_2O-CO_2 and DEA-H_2O-CO_2. *Fluid Phase Equilib.* **2008**, *263*, 131−143.
(56) Du, Y.; Rochelle, G. T. Thermodynamic modeling of aqueous piperazine / (N-(2-aminoethyl) piperazine for CO_2 capture. *Energy Procedia* **2014**, *63*, 997−1017.
(57) Shiflett, M. B.; Kasprzak, D. J.; Junk, C. P.; Yokozeki, A. Phase behavior of {carbon dioxide + [bmim] [Ac]} mixtures. *J. Chem. Thermodyn.* **2008**, *40*, 25−31.
(58) Najibi, H.; Maleki, N. Equilibrium solubility of carbon dioxide in N-methyldiethanolamine + piperazine aqueous solution: Experimental measurement and prediction. *Fluid Phase Equilib.* **2013**, *354*, 298−303.
(59) Sadegh, N.; Stenby, E. H.; Thomsen, K. Thermodynamic modelling of CO_2 absorption in aqueous N-methyldiethanolamine using extended UNIQUAC model. *Fuel* **2015**, *144*, 295−306.
(60) Mota Martinez, M. T.; Kroon, M. C.; Peters, C. J. Modeling CO_2 solubility in an ionic liquid: a comparison between a cubic and a group contribution EoS. *J. Supercrit. Fluids* **2015**, *101*, 54−62.
(61) Kundu, M.; Bandyopadhyay, S. S. Solubility of CO_2 in water + diethanolamine + N-methyldiethanolamine. *Fluid Phase Equilib.* **2006**, *248*, 158−167.
(62) Benamor, A.; Aroua, M. K. Modeling of CO_2 solubility and carbamate concentration in DEA, MDEA and their mixtures using Deshmukh-Mather model. *Fluid Phase Equilib.* **2005**, *231*, 150−162.
(63) Kim, I.; Hoff, K. A.; Hessen, E. T.; Haug-Warberg, T.; Svendsen, H. F. Enthalpy of absorption of CO_2 with alkanolamine solutions predicted from reaction equilibrium constants. *Chem. Eng. Sci.* **2009**, *64*, 2027−2038.
(64) Suleman, H.; Maulud, A. S.; Syalsabila, A. Thermodynamic modelling of carbon dioxide solubility in aqueous amino acid salt solutions and their blends with alkanolamines. *J. CO_2 Util.* **2018**, *26*, 336−349.
(65) Pakzad, P.; Mofarahi, M.; Izadpanah, A. A.; Afkhamipour, M.; Lee, C.-H. An experimental and modeling study of CO_2 solubility in a 2- amino-2-methyl-1-propanol (AMP) +N-methyl-2-pyrrolidone (NMP). *Chem. Eng. Sci.* **2018**, *175*, 365−376.
(66) Liu, H.; Chan, C.; Tontiwachwuthikul, P.; Idem, R. Analysis of CO_2 equilibrium solubility of seven tertiary amine solvents using thermodynamic and ANN models. *Fuel* **2019**, *249*, 61−72.
(67) Dey, A.; Dash, S. K.; Balchandani, S. C.; Mandal, B. Investigation on the inclusion of 1-(2-aminoethyl) piperazine as a promoter on the equilibrium CO_2 solubility of aqueous 2-amino-2-methyl-1-propanol. *J. Mol. Liq.* **2019**, *289*, 111036.
(68) Dash, S. K.; Samanta, A. N.; Bandyopadhyay, S. S. Simulation and parametric study of the post combustion CO_2 capture using aqueous 2-amino -2-methyl-1-propanol and piperazine. *Int. J. Greenh. Gas Control* **2014**, *21*, 130−139.
(69) Mathias, P. M.; Reddy, S.; Smith, A.; Afshar, K. Thermodynamic analysis of CO_2 capture solvents. *Int. J. Greenh. Gas Control* **2013**, *19*, 262−270.
(70) Kim, I.; Svendsen, H. F. Heat of absorption of carbon dioxide (CO_2) in monoethanolamine (MEA) and 2-(aminoethyl) ethanolamine (AEEA) solutions. *Ind. Eng. Chem. Res.* **2007**, *46*, 5803−5809.
(71) Carson, J. K.; Marsh, K. N.; Mather, A. E. Enthalpy of solution of carbon dioxide in (water + monoethanolamine, or diethanolamine, or N-methyldiethanolamine) and (water + monoethanolamine + N-methyldiethanolamine) at T=298.15 K. *J. Chem. Thermodyn.* **2000**, *32*, 1285−1296.
(72) Pandey, D.; Kumar Mondal, M. Thermodynamic modeling and new experimental CO_2 solubility into aqueous EAE and AEEA blend, heat of absorption, cyclic absorption capacity and desorption study for post-combustion CO_2 capture. *Chem. Eng. J.* **2021**, *410*, 128334.
(73) Chowdhury, F. A.; Okabe, H.; Shimizu, S.; Onoda, M.; Fujioka, Y. Development of novel tertiary amine absorbents for CO_2 capture. *Energy Procedia* **2009**, *1*, 1241−1248.
(74) Liang, Y.; Liu, H.; Rongwong, W.; Liang, Z.; Idem, R.; Tontiwachwuthikul, P. Solubility, absorption heat and mass transfer

studies of CO_2 absorption into aqueous solution of 1-dimethylamino-2-propanol. *Fuel* **2015**, *144*, 121−129.

(75) Ling, H.; Liu, S.; Gao, H.; Zhang, H.; Liang, Z. Solubility of N_2O, equilibrium solubility, mass transfer study and modeling of CO_2 absorption into aqueous monoethanolamine (MEA)/1-dimethylamino-2-propanol (1DMA2P) solution for post-combustion CO_2 capture. *Sep. Purif. Technol.* **2020**, *232*, 115957.

(76) Possolo, A. *Simple guide for evaluating and expressing the uncertainty of NIST measurement results*; U.S. Department of CommerceNIST Technical Note: Washington, D.C., 1900, 2015.

(77) Kumar, G.; Kundu, M. Solubility of CO_2 in aqueous blends of (N-methyl-2-ethanolamine + N-methyl-diethanolamine) and (N-methyl-2-ethanolamine + 2-amino-2-methyl-1-propanol). *J. Chem. Eng. Data* **2012**, *57*, 3203−3209.

https://doi.org/10.1021/acsomega.2c02217
ACS Omega 2022, 7, 23611−23623